Highly Linear Broadband Photonic-Assisted Q-Band ADC

Daniel J. Esman, *Student Member, IEEE*, Andreas O. J. Wiberg, *Member, IEEE*,
Nikola Alic, *Member, IEEE*, and Stojan Radic, *Member, IEEE*

Abstract—A highly linear broadband photonic-assisted analog-to-digital converter (ADC) based on high-frequency optical sampling utilizing a dual output Mach–Zehnder modulator operating with signal frequencies up to 50 GHz is presented. The pulses employed in the optical sampling were generated by a cavity-less pulse source operated at 10 GHz in preference to conventional mode-locked lasers. The optical sampling front-end greatly extends the operational frequency range of the Nyquist limited electronic digitization back-end. The performance of the sampling system is characterized with 7.1 effective number of bits (ENOBs) at 40 with 5 GHz fully accessible bandwidth, and greater than 99 dB·Hz$^{2/3}$ spurious free dynamic range for the 30–40 GHz frequency range. Furthermore, more than 8 ENOB was achieved by reducing the effective bandwidth to 1 GHz with a digital filter, demonstrating the additional advantage of using a higher sampling rate compared to previous demonstrations. A new figure of merit of photonic-assisted sub-sampled ADCs is also presented accompanied with a comparison to previous implementations.

Index Terms—Analog-digital conversion, detection, microwave photonics, optical data processing, optical fiber communications, sampling, sub-sampling.

I. INTRODUCTION

THE widespread adoption of digital signal processing (DSP) techniques in application domains spanning communication and sensing in commercial, and defense applications mandate analog to digital conversion (ADC) functionality operable on the femtosecond time-scale and with uncompromised, high resolution. Currently, the A-to-D performance represents the limiting factor to the successful high speed DSP implementation and utility. The ADC performance, in turn, is limited by its underlying signal to noise ratio (SNR), linearity, aperture jitter, and sampling ambiguity (the width of the sampling gate/aperture) [1]. Prominently, recent advances have shown that these limitations can largely be removed, or mollified by the use of photonic assisted ADCs, thereby circumventing the shortcoming associated with conventional purely-electronic devices [2]. Indeed, photonic assisted ADCs have become a prudent means to improving high accuracy in high speed signal detection and/or sensing. The basic advantage of these hybrid architectures lay in their ability to effectively combine the fast sampling techniques of photonics with the high processing complexity capable electronics.

In particular, the photonic assisted ADCs have been shown to be directly applicable in microwave and millimeter wave down-conversion schemes [3]–[6]. In fact, the last down-conversion approach has recently been implemented in field trials for a fully photonics based radar [7]. In these high frequency systems, carrier frequencies can typically be orders of magnitude greater than their signal carrying bandwidth. As a result, the carrier frequency down conversion is useful to reduce the requirements of the backend ADC. This, what is often referred to as conventional down-conversion, is usually achieved by a local oscillator (LO) and a mixer that translate the signal to an intermediate frequency as depicted in Fig. 1(a). However, the reliance on a single LO implicitly assumes the knowledge about the exact position of the signal carrier frequency (in order to achieve the down-conversion to baseband), which may not be the case in applications such as RADAR, thus in effect preventing the detection of signals of arbitrary, or varying carrier frequency. As a simpler alternative, the down conversion can be performed directly by means of subsampling (at a rate lower than two times the carrier frequency), effectively taking advantage of aliasing to down-convert the unknown microwave or millimeter-wave frequency to the first Nyquist zone, thereby eliminating the need for exact knowledge of the signal (or the LO) position. As stated above, the conceived method is applicable only for signals whose bandwidth is smaller than half of the (sub) sampling rate. The latter method can be put into practice by means of photonic assisted ADCs that can directly down convert a signal with high fidelity and wide bandwidth sampling, thus allowing complex digitization steps to be completed in electronics at a lower rate, all the while without the need for an LO matching the signal carrier frequency. Following their functionality, these devices are often denoted to as the microwave-to-digital converters (MDC) [3]. A block diagram of the photonic MDC is shown in Fig. 1(b). For both defense and commercial applications, an MDC also has an added advantage over conventional LO down-conversion [8], in that the signal can be modulated onto optical pulses and transported over fiber to a (possibly remote) processing location. The last scenario has obvious advantages with respect to the conventional technique (shown in Fig. 1(a)), which requires detection hardware to be at the antenna location due to the high loss associated with radio frequency (RF) waveguides [8], increasing complexity, as well as the size and weight of the bulky RF waveguides in comparison to optical fiber waveguides [8].
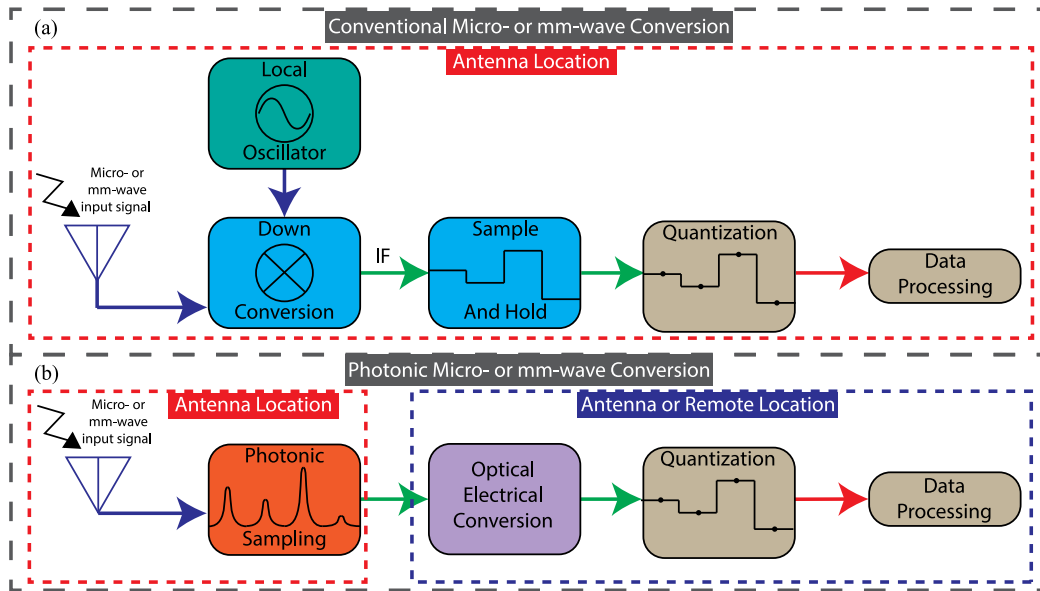
Fig. 1.   (a) Conventional microwave or millimeter wave conversion. (b) Photonic microwave or millimeter wave conversion.

Additionally, the detectible (i.e., reconstructible) bandwidth of the MDC can be further increased with the introduction of the so-called scaled sampling [6]. The sampling rate scaling can be accomplished through parallelization, in which optical pulses are replicated into e.g. multiple wavelengths via four-wave mixing and then temporally interleaved through the sampling gate, as previously demonstrated in parametric gates [9], [10], allowing for full reconstruction of arbitrarily high frequency signal inputs.

In particular, the sampling gate presented in this work is realized by employing a dual output Mach–Zehnder modulator (DO-MZM) allowing for the direct down conversion of millimeter waves in the Q-band (between 33 and 50 GHz [11]) with maximum resolution. In the employed approach, both complementary outputs of the DO-MZM will share the same common-mode noise. Thus, utilizing a parallel receiver architecture, quantization and subsequent subtraction of these complementary outputs yields a reduction in the laser relative intensity noise, as well as an improvement in the SNR, and reduction of modulator nonlinearities [12]–[14]. A further modulator nonlinearity reduction can be achieved by adopting a well known arcsine-based equalization of the transfer function of the DO-MZM [13], [14], ultimately cancelling the second and third order distortions common to both optical paths. Moreover, the available higher sampling rate allows for implementation of DSP filters to match the desired bandwidth, and consequently reducing the bandwidth of the noise, resulting in a higher SNR [21], enabling signal capturing accuracy beyond what has previously been achievable.

Here we present more extensive results over the preliminary characterization introduced in [15] that are a significant leap in performance in terms of the SNR and the available bandwidth with respect to the previous demonstrations, e.g., [13], [14], [16]–[18]. In particular, the constructed photonic ADC preprocessor performance was rigorously characterized at a record of 7.1 (8.0) and 6.7 (7.4) ENOBs at 39.49 and 49.49 GHz, with 5 GHz (1 GHz) bandwidth, as well as with 99 dB·Hz$^{2/3}$ spurious-free dynamic range (SFDR) for the 30–40 GHz range, demonstrating the unprecedented highly linear, high accuracy ADC/MDC. These results are compared with previous implementations using a new figure of merit (FOM) for photonic sampled ADC, and they show the highest FOM value for signals up to 50 GHz, to the best of the authors knowledge.

The remainder of this paper is organized as follows. In Section II, the operational principles of the sampling scheme are discussed. In Section III, the experimental sampling setup is described. The experimental results and performance analysis are presented in Section IV. A new FOM is discussed and presented in Section V with a comparison to other photonic-assisted ADC implementations. Concluding remarks follow in Section VI.

II. PRINCIPLE OF OPERATION

The photonic down conversion technique demonstrated here is based on the well known principle of an RF signal being imprinted onto short optical pulses using an electro-optical modulator. The short optical pulse creates a narrow temporal sampling gate event with the energy of the pulses after sampling proportional to the amplitude of the incoming signal at that instance. In this case, the optical pulse rate is purposely chosen to be less than twice the RF carrier signal rate, thus, effective down conversion of the RF signal is achieved after passing through the system, as described above and in Fig. 1(b). In our implementation, a DO-MZM is used to perform the sampling process, together with an optical cavity-less pulse source. The short optical pulses generated from the cavity-less pulse source are synchronized with a back-end that converts the signal from the optical to electrical, and subsequently to the digital domain. Before final digitization, an electrical front-end employs several techniques to refine the signal to improve performance and reduce
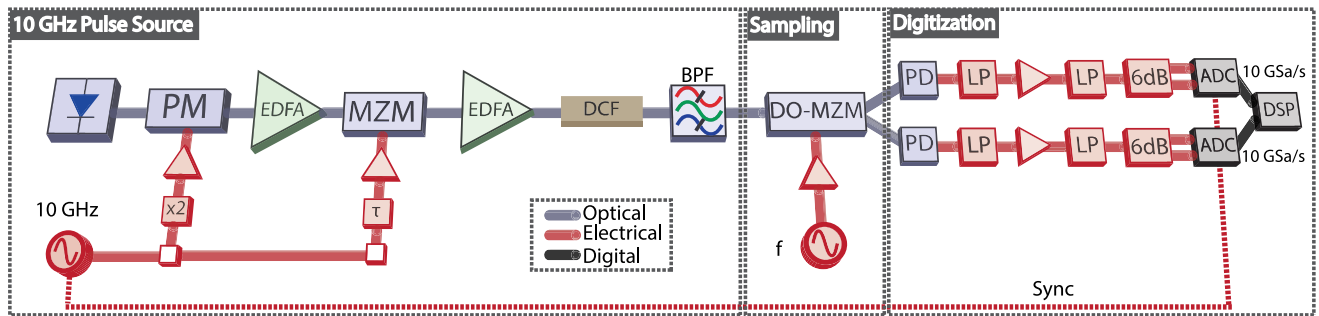
Fig. 2.   Experimental setup. PM: Phase modulator, EDFA: Erbium doped fiber amplifier, τ: Delay, MZM: Mach–Zehnder modulator, DCF: Dispersion compensating fiber, BPF: Band pass filter, DO-MZM: Dual output Mach–Zehnder modulator, PD: photodiode, LP: Low pass filter.

the requirements of the final electronic ADC. An overview of the photonic sampling system is shown in Fig. 2.

The principle of the DO-MZM sampling architecture combines several techniques in the optical domain to improve the overall performance of the system. First, the sampling pulses used were generated with a cavity-less pulse source in preference to conventional mode-locked lasers [17], [19]. The 10 GHz pulse source implemented in this paper was an improved design over the 2 GHz pulse source utilized previously [17], [20]. The main improvement was the ability to generate these pulses with fewer components and reduced loss, thus allowing for fewer Erbium doped fiber amplifiers (EDFA), resulting in less amplified spontaneous emission (ASE) limiting the SNR of the pulse source. Furthermore, the EDFAs in the pulse source were driven in deep saturation to reduce any additive noise in the amplification process.

In addition, the DO-MZM sampling architecture presented here also applied techniques in the electronic and digital domains to improve the sampling fidelity. Namely, the bandwidth of the input signal (assumed to be 1 GHz or less) will be oversampled by the 10 GHz optical pulse source after the signal is downconverted, thus allowing for an improvement in performance of the digitization step by low- or band-pass filtering [21]. In order to emulate an integrate and dump and track and hold circuit in the electronic backend, following the photo-detectors, 5 GHz low pass (LP) filters were applied to the 10 GSa/s pulses, with 5 GHz RF bandwidth, to cut any excess noise from the photo-detectors and to significantly reduce the jitter requirements on the subsequent ADC [22]. Also, each complementary electrical path was split into two, and all four paths were digitized with independent electrical digitizers synchronously. In particular, after capturing, each of the two channels (essentially carrying identical data) were added, yielding a 3 dB SNR improvement on each complimentary arm of the electrical backend while maintaining a much less complex DSP step than time interleaving [21]. Additionally, since both complementary outputs are synchronously oversampled with high fidelity (compared to the signal bandwidth), a DSP step can be taken to undo the sinusoidal transfer function of the DO-MZM, as mentioned above, mitigating nonlinearities and noise common to both complementary optical paths. Combining all these techniques in the optical, electrical and digital domains produces an ultrahigh fidelity photonic assisted ADC processor, capable of down

converting high frequency signals while maintaining high linearity and digitization accuracy.

III. EXPERIMENT

The experimental setup is shown in Fig. 2. The 10 GHz pulse source was driven with a 20 dBm continuous wave (CW) distributed feedback laser seed centered at 1564.7 nm. A chirp was then imposed onto the CW seed using a phase modulator (PM) driven at 20 GHz, derived from a doubled high quality master 10 GHz RF tone. The master seed was subsequently amplified with an EDFA, operated in the deep saturation regime, ensuring a low noise-accompanied amplification. The chirped seed was then passed through a MZM driven with the master 10 GHz tone compressed in a saturated modulator driver, resulting in a repetitive 10 GHz pulse train. After another amplification stage, the chirped pulses were compressed in a 31.5 m-long segment of standard dispersion compensating fiber (DCF), ultimately yielding a sought after 3.5 ps wide, 13.5 dBm strong 10 GHz pulse stream. Finally, out of band ASE was suppressed by an optical band pass filter. The 10 GHz cavity-less pulse source used possessed a measured –123.7 dBc/Hz single sided phase noise level at 10 kHz offset.

The short pulses were next routed to a DO-MZM in which the sampling operation was performed. The DO-MZM was driven with an RF test probe (sinusoid) at various frequencies to rigorously measure ENOB [23], or, alternatively, with two RF test probes (sinusoids) with 200 MHz separation for SFDR characterization. After the sampling operation, the two complementary paths, each with approximately 5 dBm average power, were sent to 20 GHz photo-diodes for optical to electrical conversion. The electronic signals were then LP filtered with 5 GHz bandwidth, amplified and subsequently passed through another pair of 5 GHz LP filters. Both electronic signals were power split and sent to 2 real-time oscilloscope channels, performing a (parallel) sampling operation. The conceived arrangement created a 7-ENOB capable backplane digitizer at 10 GSa/s for each complementary channel. In the experiment, the digitizers were strictly synchronized with the pulse source, and the path lengths from the DO-MZM to the electronic digitizers were matched to within 20 ps to ensure simultaneous capturing. The digitized output was then processed using DSP. The DSP, in addition to the SNR-increasing summation mentioned above, consisted
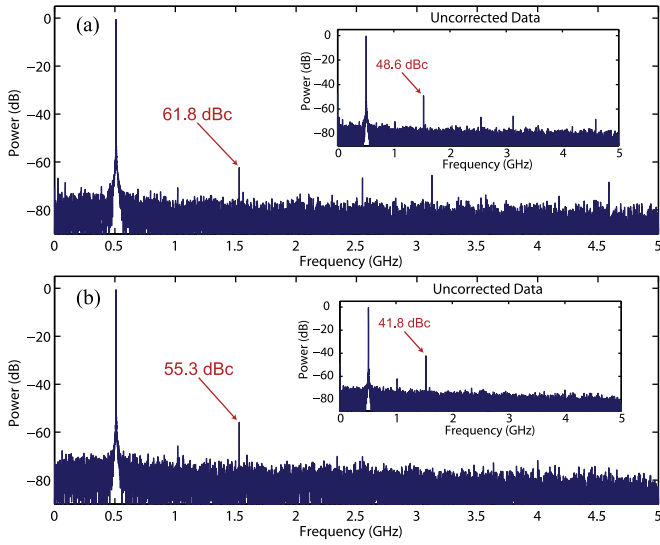
Fig. 3. FFT of captured single tone inputs with frequencies of (a) 39.49 GHz and (b) 49.49 GHz. Figure insets represent uncorrected data at the same frequencies.

of applying a linearization method based on [13], [14]. This equalization method first calibrated the complementary amplitudes and offsets, and finally employed an arcsine equalization to their difference in order to compensate for the well-known sinusoidal transfer function of the system [13], [14]. Ideally, this calibration could be done on a training sequence only once. However, due to manual bias control and manual polarization alignment into the modulators in the experiment, the calibration needed to be done on a short training sequence at the beginning of each capture.

IV. EXPERIMENTAL RESULTS

A. Single Tone Characterization

The performance of the system was first characterized with a single tone input sinusoid with frequency varying from 30–50 GHz to estimate the resolution in terms of ENOB. The characterization was performed with a test signal, modulated onto optical pulses using the DO-MZM, biased at the quadrature point, and finally, each complementary output was detected with a photodiode and digitized by parallel electronic backplanes. The digitized, transfer function compensated fast Fourier transform (FFT) of the 20k sub-rate samples of the output is shown in Fig. 3 with input frequencies 39.49 and 49.49 GHz. We note that the aliasing effect of sub-rate sampling makes the frequency appear at 510 MHz. The uncorrected, raw data are also shown in the figure insets. The resultant compensation leads to a greater than 13 dB decrease in the third order distortion resulting from the nonlinearities in the DO-MZM. As seen in Fig. 3, the small remnant spurs are due to the non-identical nonlinearities that are present in each of the complementary paths, but are not the major limiting factor in the work presented here.

The rigorously quantified high resolution of the constructed MDC/ADC over the full range from 30 to 50 GHz is shown in Fig. 4. As seen in Fig. 4, the 10 GSa/s system performed

with 7.1 ENOBs at 30.49 and 39.49 GHz, and 6.7 ENOBs at 49.49 GHz with full 5 GHz bandwidth. In addition to the natural overall descending resolution of the MDC two local drops in performance are recognized in the recorded characteristic. The drop in performance near 35 and 45 GHz is due to the particular electronic ADC frequency response at the edge of the Nyquist bandwidths, and has no bearing on the concept employed. On the other hand, the drop in performance from the 30–40 GHz range to the 40–50 GHz range is attributed to the frequency response of the DO-MZM and the increased sampling source requirements with frequency, both of which can also be improved further.

Moreover, most MDC applications require a bandwidth significantly narrower than 5 GHz. Consequently an additional system performance was evaluated at a bandwidth of 1 GHz, with results also shown in Fig. 4. The narrower bandwidth of the digitized frequency window (i.e., 1 GHz) was characterized with performance of as much as 8.1, 8.0 and 7.4 ENOBs at 31.51, 39.49 and 49.49 GHz, respectively. This is, to the best of the authors' knowledge, a full 1 ENOB better than any reported ADC or MDC at 40 GHz and 50 GHz with 1 GHz or higher bandwidth, to date.

B. Two-Tone Characterization

The system was also characterized using a two-tone stimuli for a comprehensive linearity evaluation of the performance. In the measurements, two-tones with a 200 MHz separation were generated and used as an input signal for a range of frequencies from 30 to 41 GHz. The narrower frequency characterization span for the two-tone tests (i.e., 30–40 GHz, as opposed to 30–50 GHz used in single tone ENOB measurements) was imposed by the unavailability of a frequency combiner and a second RF synthesizer beyond 40 GHz.

The digitized, transfer function compensated FFT of the 20k sub-rate samples of the output is shown in Fig. 5, with input frequencies of 31.1 and 31.3 GHz, as well as for 41.1 and 41.3 GHz doublet with input electrical power of 11.5 and 17.5 dBm, respectively. The uncorrected, raw data is also shown as figure insets. The third order intercept point measurement is shown in Fig. 6(a) and (b) for 31.1 and 31.3 GHz, and 41.1 and 41.3 GHz, respectively, where the electrical input power was increased from –2 to 19 dBm. For these two frequency sets, a third order SFDR of 99.3 and 100 dB·Hz$^{2/3}$ were measured. Also, a third order SFDR of over 99 dB·Hz$^{2/3}$ was measured across the 30–41 GHz range in which results are presented in Fig. 6(c). We note that the SFDR measurements represent conservative estimates, in that they are calculated as the smaller measured value of the two signal powers to the strongest value of the two third order intermodulation distortions. This corresponds to over 5.4 two-tone ENOB over this range with 5 GHz bandwidth noise. The authors note that because a fixed fill ratio was maintained for both single and two-tone measurements, there is a 1 ENOB difference between the single and two-tone measurements due to 6 dB lower power per tone in the two-tone case. As a result, the two-tone measurements and single-tone measurements are in good agreement if one also considers that the SFDR was measured as a conservative value, i.e., the lowest of the fundamental
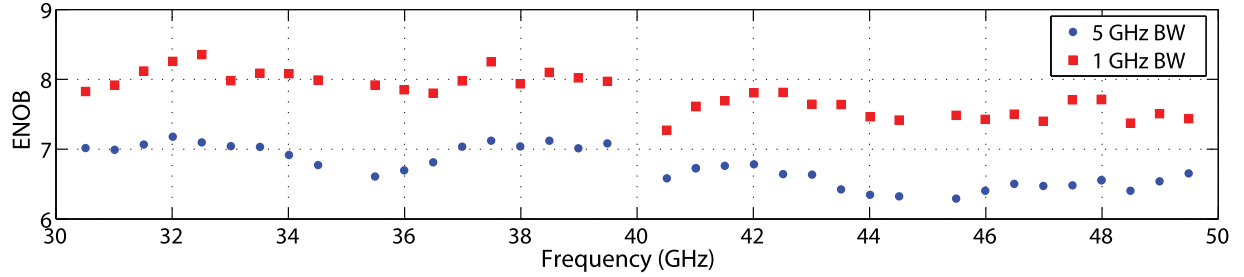
Fig. 4.   ENOB as a function of input signal frequency for 5 GHz bandwidth and 1 GHz bandwidth.
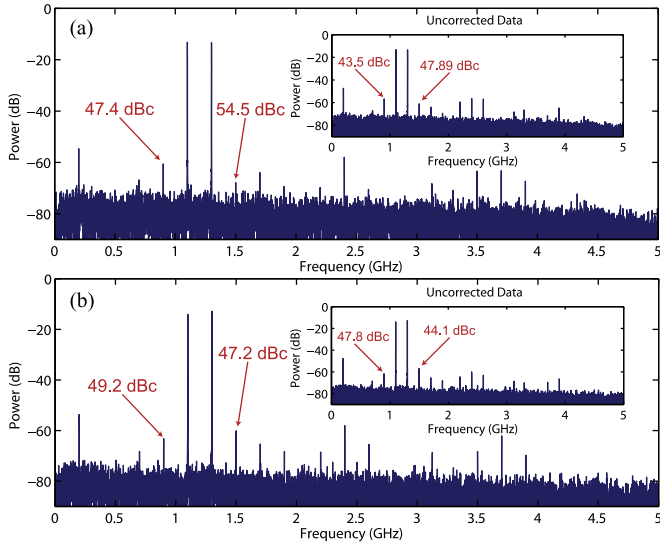

Fig. 5.   FFT of captured two-tone inputs with frequencies and RF powers into the DO-MZM of (a) $f_1 = 31.1$ GHz, $f_2 = 31.3$ GHz and $P_{in} = 11.5$ dBm and (b) $f_1 = 41.1$ GHz, $f_2 = 41.3$ GHz and $P_{in} = 17.5$ dBm. Figure insets represent uncorrected data of the same frequencies and powers.
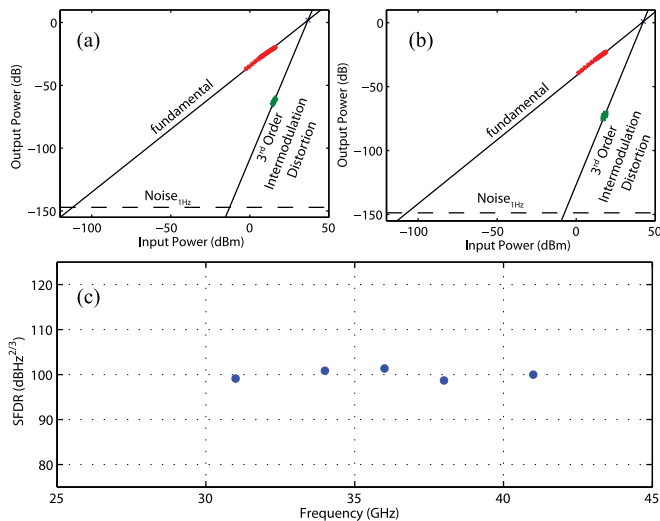

Fig. 6.   Fundamental and third order intermodulation tone powers for (a) $f_1 = 31.1$ GHz, $f_2 = 31.3$ GHz and (b) $f_1 = 41.1$ GHz, $f_2 = 41.3$ GHz. (c) SFDR as a function of input signal frequency.

tones compared with the strongest intermodulation distortion tones, placing the actual two-tone ENOB close to 7 for the 30–41 GHz range with 5 GHz noise bandwidth.

V. DISCUSSION: NEW FOM

The ADC comparison first defined in [1] has long been used to compare performance measures of Nyquist sampled ADCs. However, the subsampled ADCs/MDCs possess an additional feature that needs to be taken into account for a rigorous comparison. For instance, a subsampled system performing with 8 ENOB at 20 GHz signal frequency and with a 10 GHz operational bandwidth is a superior architecture than one operating with the same resolution (i.e., 8 ENOB) and carrier frequency (i.e., 20 GHz) operating over 10 MHz available bandwidth. As a result, we introduce a new FOM which, in our opinion is better suited to sub-sampled ADCs/MDCs. The proposed FOM encapsulates the performance of single tone input ADCs, based on ENOBs, N, operational bandwidth, Δf, and signal carrier frequency, f_c. In particular, the FOM is defined as follows:

$$\text{FOM} = 2^N \sqrt{\Delta f} f_c. \tag{1}$$

It should be emphasized that a system characterized at f_c with available bandwidth Δf should have the same FOM as the same system characterized at $2f_c$, Δf (if jitter limited), or at f_c, $4\Delta f$ (if noise limited), as N should reduce by 1 in either latter case. Thus, this FOM correctly includes the bandwidth that is missing from the analysis of Nyquist-sampled ADCs in [1]. Finally, as shown in Fig. 7, taking the all-important (for sub-sampled ADCs) operational bandwidth parameter into account the constructed system performs more than 100% better than the systems in [6], [13], [14], [16]–[18], [20]–[26] as well as any system covered in the photonic assisted ADC reviews by [16], [27]. In addition, this system performs comparably to [28], which used the same optical cavity-less pulse source and a similar electrical channel backplane scheme, demonstrating the effectiveness of these techniques.

VI. CONCLUSION

We have designed and tested the first 40 GHz ADC processor operating with 8 ENOB resolution, based on high frequency optical sampling relying on a DO-MZM. Rigorous characterization was performed with both a single and two-tone input to measure the IEEE standard ENOB and the SFDR performances, in the Q-band, respectively. This characterization confirmed
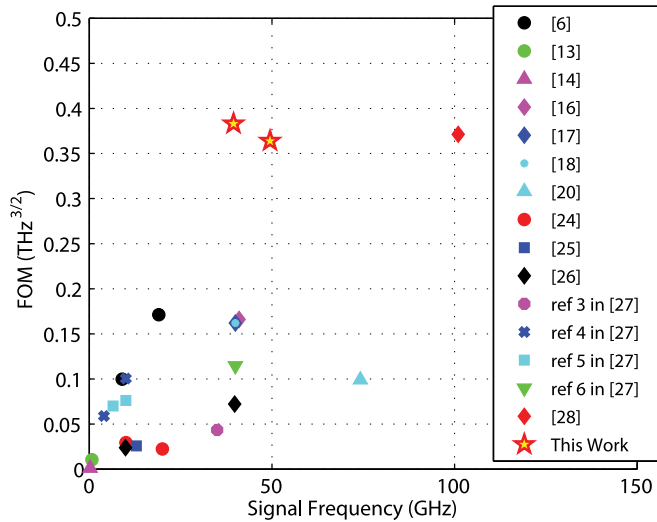
Fig. 7. FOM as a function of input signal frequency for existing photonic assisted ADC architectures including 7.1 ENOB at 39.49 GHz and 6.7 ENOB at 49.49 GHz with 5 GHz bandwidth demonstrated in this work.

the exceedingly linear, high resolution performance with 7.1 and 6.7 ENOBs with 5 GHz operational bandwidth and 8.0 and 7.4 ENOBs over 1 GHz MDC bandwidth at signal frequencies of 39.49 and 49.49 GHz, respectively. Additionally, a third order SFDR of more than 99 dB·Hz$^{2/3}$ over the 30–41 GHz range was measured in the two-tone-based intermodulation characterizations. To the best of the authors' knowledge, this is the highest performing ADC/MDC in terms of the ENOBs at the given frequencies and the newly introduced sub-sampled ADC relevant FOM. The demonstrated system perfectly fits applications in microwave and millimeter-wave direct down conversion of high practical interest and at the immediately available sub-rate sampling rates. Finally, it ought to be emphasized that the demonstrated system is by no means limited to sampling speeds explored in this work and can successfully be scaled to A/D operation at virtually arbitrary signal frequencies.

REFERENCES

[1] R. H. Walden, "Analog-to-digital converter survey and analysis," *IEEE J. Sel. Areas Commun.*, vol. 17, no. 4, pp. 539–550, Apr. 1999.

[2] G. C. Valley, "Photonic analog-to-digital converters," *Opt. Exp.*, vol. 15, pp. 1955–1982, 2007.

[3] T. Clark, "Photonic microwave-to-digital-conversion," presented at the IEEE Photon. Conf., 2013, Paper WC4.1, pp. 422–423.

[4] A. J. Seeds and K. J. Williams, "Microwave photonics," *J. Lightw. Technol.*, vol. 24, no. 12, pp. 4628–4641, Dec. 2006.

[5] J. Capmany and D. Novak, "Microwave photonics combines two worlds," *Nature Photon.*, vol. 1, pp. 319–330, 2007.

[6] D. J. Esman, A. O. J. Wiberg, E. Temprana, Y. Myslivets, P. P. Kuo, N. Alic, and S. Radic, "A fully frequency referenced parametric polychromatically sampled analog-to-digital conversion," presented at the Opt. Fiber Commun. Conf., San Francisco, CA, USA, 2014, Paper TH3D.4.

[7] P. Ghelfi, F. Laghezza, F. Scotti, G. Serafino, A. Capria, S. Pinna, D. Onori, C. Porzi, M. Scaffardi, A. Malacarne, V. Vercesi, E. Lazzeri, F. Berizzi, and A. Bogoni, "A fully photonics-based coherent radar system," *Nature*, vol. 507, pp. 341–345, 2014.

[8] C. H. Cox, E. I. Ackerman, and G. E. Betts, "The role of photonic and electronic gain in the design of analog optical links," presented at the IEEE Avion. Fiber-Opt. Photon. Conf., Minneapolis, MN, USA, 2005, Paper TuA1, pp. 71–72.

[9] M. Sköld, M. Westlund, H. Sunnerud, and P. A. Andrekson, "100 GSample/s optical real-time sampling system with nyquist-limited bandwidth," presented at the 33rd Eur. Conf. Exhib. Opt. Commun. - Post-Deadline Papers, Berlin, Germany, 2007.

[10] A. O. J. Wiberg, C.-S. Bres, B. P.-P. Kuo, J. M. C. Boggio, N. Alic, and S. Radic, "Multicast parametric synchronous sampling of 320-Gb/s return-to-zero signal," *IEEE Photon. Technol. Lett.*, vol. 21, no. 21, pp. 1612–1614, Nov. 2009.

[11] FCC Bulletin 70, "Millimeter wave propagation: Spectrum management implication," (1997, Jul.). [Available]: www.fcc.gov/encyclopedia/oet-bulletins-line#70

[12] K. J. Williams, L. T. Nichols, and R. D. Esman, "Photodetector nonlinearity limitations on a high-dynamic range 3 GHz fiber optic link," *J. Lightw. Technol.*, vol. 16, no. 2, pp. 192–199, Feb. 1998.

[13] R. C. Williamson, R. D. Younger, P. W. Juodawlkis, J. J. Hargreaves, and J. C. Twichell, "Precision calibration of an optically sampled analog-to-digital converter," presented at the Dig. IEEE LEOS Summer Top. Meeting Photon. Time/Freq. Meas. Control, Vancouver, BC, Canada, 2003, Paper MC4.2.

[14] P. W. Juodawlkis, J. C. Twichell, G. E. Betts, J. J. Hargreaves, R. D. Younger, J. L. Wasserman, F. J. O'Donnell, K. G. Ray, and R. C. Williamson, "Optically sampled analog-to-digital converters," *IEEE Trans. Microw. Theory Tech.*, vol. 49, no. 10, pp. 1840–1853, Oct. 2001.

[15] D. J. Esman, A. O. J. Wiberg, N. Alic, and S. Radic, "High resolution broadband photonic sampled ADC: 8.0 ENOB at 40 GHz," presented at the. Optoelectron. Commun. Conf. Australian Opt. Fibre Technol., Melbourne, Vic., USA, 2014, Paper TU3E-1.

[16] A. Khilo, S. J. Spector, M. E. Grein, A. H. Nejadmalayeri, C. W. Holzwarth, M. Y. Sander, M. S. Dahlem, M. Y. Peng, M. W. Geis, N. A. DiLello, J. U. Yoon, A. Motamedi, J. S. Orcutt, J. P. Wang, C. M. Sorace-Agaskar, M. A. Popović, J. Sun, G. R. Zhou, H. Byun, J. Chen, J. L. Hoyt, H. I. Smith, R. J. Ram, M. Perrott, T. M. Lyszczarz, E. P. Ippen, and F. X. Kärtner, "Photonic ADC: Overcoming the bottleneck of electronic jitter," *Opt. Exp.*, vol. 20, pp. 4454–4469, 2012.

[17] A. O. J. Wiberg, L. Liu, Z. tong, E. Myslivets, V. Ataie, B. P. P. Kuo, N. Alic, and S. Radic, "Photonic preprocessor for analog-to-digital converter using a cavity-less pulse source," *Opt. Exp.*, vol. 20, pp. B419–B427, 2012.

[18] A. H. Nejadmalayeri, M. E. Grein, A. Khilo, J. Wang, M. Y. Sander, M. Peng, C. M. Sorace, E. P. Ippen, and F. X. Kaertner, "A 16-fs aperture-jitter photonic ADC: 7.0 ENOB at 40 GHz," presented at the Conf. Lasers Electro-Opt. - Laser Appl. Photonic Appl., Baltimore, MD, USA, 2011, Paper CThI6.

[19] A. O. J. Wiberg, C.-S. Brès, B. P.-P. Kuo, E. Myslivets, and S. Radic "Cavity-less 40 GHz pulse source tunable over 95 nm," presented at the 35th Eur. Conf. Opt. Commun., Vienna, Austria, 2009, Paper 5.2.3.

[20] A. O. J. Wiberg, D. J. Esman, L. Liu, Z. Tong, E. Myslivets, N. Alic, and S. Radic, "Demonstration of 74 GHz parametric optical sampled analog-to-digital conversion," presented at the 39th Eur. Conf. Opt. Commun., London, U.K., 2013, Paper Tu.1.C.1.

[21] R. Reeder, M. Looney, and J. Hand, "Pushing the state of the art with multichannel A/D converters," *Analog Dialogue*, vol. 39, pp. 7–10, 2005.

[22] T. D. Gathman and J. F. Buckwalter, "An integrate-and-dump receiver for high dynamic range photonic analog-to-digital conversion," presented at the IEEE 12th Top. Meeting Silicon Monolithic Integr. Circuits RF Syst., Santa Clara, CA, USA, 2012, Paper TU1C-4.

[23] *The Institute of Electrical and Electronics Engineers*, IEEE Std. 1241–2000, 2001.

[24] D. R. Reilly, S. X. Wang, and G. S. Kanter, "Optical under-sampling for high resolution analog-to-digital conversion," presented at the IEEE Avionics Fiber-Opt. Photon. Conf., San Diego, CA, USA, 2011, Paper TuD3.

[25] O. Golani, L. Mauri, F. Pasinato, C. Cattaneo, G. Consonnni, S. Balsamo, and D. M. Marom, "High-resolution, photonically-sampled, analog-to-digital conversion employing spatial oversampling," presented at the Opt. Fiber Commun. Conf., San Francisco, CA, USA, 2014, Paper TH3D.1.

[26] F. Laghezza, F. Scotti, P. Ghelfi, and A. Bogoni, "Jitter-limited photonic analog-to-digital converter with 7 effective bits for wideband radar applications," presented at the Proc. IEEE Radar Conf., Ottawa, ON, USA, 2014.

[27] F. X. Kartner, A. Khilo, and A. H. Nejadmelayeri, "Progress in photonic analog-to-digital conversion," presented at the Opt. Fiber Commun. Conf., Anaheim, CA, USA, 2013, Paper OTh3D.5.

[28] D. J. Esman, A. O. J. Wiberg, M.-H. Yang, L. Liu, B. P.-P. Kuo, N. Alic, and S. Radic, "Photonic parametric sampled analog-to-digital conversion at 100 GHz and 6 ENOBs," presented at the 40th Eur. Conf. Opt. Commun., Cannes, France, 2014, Paper Mo.3.5.6.

Daniel J. Esman (S'13) received the B.A. degree in physics and mathematics from Kalamazoo College, Kalamazoo, MI, USA. He received the M.S. degree in photonics from the Department of Electrical and Computer Engineering, University of California San Diego, La Jolla, CA, USA, in 2014. From 2011 to 2012, he worked as a Junior Engineer at PriTel, Inc.

He is a Predoctoral Researcher at the Department of Electrical and Computer Engineering, University of California, San Diego. His research interests include microwave photonic systems and radar/EW signal processing.

Nikola Alic (S'00–M'06) received the B.S. degree in optoelectronics from the Belgrade School of Electrical Engineering, Belgrade, Serbia, in 1998. He received the M.S. and Ph.D. degrees in photonics from the Department of Electrical and Computer Engineering, University of California San Diego, La Jolla, CA, USA, in 2001 and 2006, respectively, for his pioneering work on the role of electronic equalization in optical communications. After graduation, he served as a Junior Scientist at the "Vinca" Institute of Nuclear Sciences in Belgrade, Serbia, where he worked on solitonic pulse compression in nonlinear fiber arrays. He is currently a Research Scientist at the California Institute of Telecommunications and Information Technologies. His research interests include equalization and coding theory in optical communications, high-speed transmission, detection theory, fiber optic parametric amplifiers, and all-optical signal processing.

Andreas O. J. Wiberg (S'04–M'08) received the M.Sc. degree in engineering physics in 2002, the Licentiate degree in electrical engineering in 2005, and the Ph.D. degree in electrical engineering in 2008, all from Chalmers University of Technology, Gothenburg, Sweden. His graduate research has mainly focused on Microwave Photonic systems and optical millimeter-wave and terahertz generation, transmission and detection.

From 2008 to 2013, he was with the Photonics System Group at the Department of Computer and Electrical Engineering, University of California San Diego, La Jolla CA, USA. He is currently with the California Institute of Telecommunications and Information Technologies, La Jolla. His current research interests include applications of parametric effects in optical fibers, including high-speed signal generation, optical pulse generation, all-optical sampling, multicasting, ultrafast optical signal processing of digital and analog signals, analog-to-digital-conversions and broadband microwave and mm-wave channelization.

Dr. Wiberg has published more than 30 articles in refereed journals, and serves on the committee for Microwave Photonics at the IEEE Photonics Conference.

Stojan Radic received the B.S. degree in electrical engineering from the University of Belgrade, Belgrade, Serbia, and the M.S. and Ph.D. degrees from the Institute of Optics, University of Rochester, Rochester, NY, USA, in 1990, 1992, and 1995, respectively. Immediately thereafter, he served as a Scientist at the Institute of Optics, investigating nonlinear periodic structures and low-threshold optical switching. During 1997–1998, he held a Senior Scientist position at Corning Photonics Division. He joined Bell Laboratories Lightwave Systems Research Department in 1998 as a Member of the technical staff, where he served until 2003. He is currently a Professor of electrical engineering at the University of California San Diego, La Jolla, CA. Immediately prior to coming to the Jacobs School of Engineering at UCSD, he held a chaired position at Duke University.

Dr. Radic has published more than 100 articles in refereed journals, and serves on committees for Optical Fiber Communication, Conference on Lasers and Electro-Optics and Optical Amplifiers and their Applications, Coherent Optical Technologies and Applications conferences. His interests include parametric amplification with signal processing, ultradense bidirectional networking, and novel signaling formats.